Microscopic Organic Analysis Using Two-Step Laser Mass Spectrometry: Application to Meteoritic Acid Residues

Laurie J. Kovalenko, Claude R. Maechling, Simon J. Clemett, Jean-Michel Philippoz,† and Richard N. Zare*

Department of Chemistry, Stanford University, Stanford, California 94305

Conel M. O'D. Alexander

McDonnell Center for the Space Sciences, Washington University, St. Louis, Missouri 63130

We have developed a microanalytical instrument to analyze the organic constituents of particulates and inhomogeneous samples with a spatial resolution of approximately 40 μm. Our method, two-step laser desorption/laser ionization mass spectrometry (L^2MS), uses an infrared laser to volatilize constituent molecules intact and an ultraviolet laser to ionize desorbed molecules in a selective manner with little or no fragmentation. In particular, our instrument is currently tuned to detect polycyclic aromatic hydrocarbons (PAHs), which have a strong absorption cross section at the ionization laser wavelength of 266 nm. The detection limit of our instrument is approximately 8 fmol for the compound coronene ($C_{24}H_{12}$). We demonstrate the use of this instrument to analyze acid residues from six meteorites; the samples consist of particles that are about 200 μm in diameter. Quantitative and qualitative trends in PAH composition are identified for different classes of meteorites. Significant differences are seen between the carbonaceous and ordinary chondrites. Moreover, within a single class of ordinary chondrites we see an increase in alkylation with increasing petrographic type (thermal metamorphism).

INTRODUCTION

Although the elemental analysis of particulates and samples that are inhomogeneous on a microscopic scale is a highly-developed technology, the organic analysis of such samples presents a challenge because of thermal fragility. To take advantage of sensitive gas-phase techniques, such as mass spectrometry, the sample must be volatilized; however, traditional evaporation methods, such as resistive heating, often result in decomposition rather than volatilization of thermally labile compounds. Moreover, the smaller the sample size or the finer the heterogeneity, the greater the need for highly localized heating.

In recent years several sensitive techniques for the organic analysis of microscopic quantities of solid samples have been developed. Methods, such as secondary ionization mass spectrometry (SIMS)[1,2] and laser microprobe mass analysis (LAMMA),[3,4] cause the ejection of ions from the sample by bombardment with a high-energy beam consisting of ions in the former method and photons in the latter. The ion and laser beams can be focused onto the sample, enabling microscopic analysis of samples. Briggs[5] has demonstrated the use of static or low-dose SIMS for the microanalysis of heterogeneous polymeric surfaces, while Gillen et al.[6] have successfully applied dynamic or high-dose SIMS to the analysis of organic molecules deposited on a conducting surface. The laser microprobe technique avoids one problem inherent in SIMS, charging of insulator samples. Novak et al.,[7] and Wilk and Hercules[8] have applied LAMMA to the mapping of a heterogeneous distribution of organic molecules on organic surfaces.

Typically, the severe conditions necessary to attain both ejection and ionization in one step often result in fragmentation of the constituent molecules. Although the presence of fragment peaks in a mass spectrum can be an asset in the structural determination of samples consisting of one compound, it can be a liability in the interpretation of mass spectra of samples consisting of a mixture of compounds. In addition, these one-step methods often generate mass spectra containing interfering ion signals from the matrix material.[9] Furthermore, the majority of particles ejected from the sample are neutral,[10,11] which may limit the sensitivity of these techniques.

Increased ion yield can be obtained by using a two-step method, where the desorption of neutral molecules in the first step is followed by gas-phase ionization in the second; moreover, the less severe conditions required for desorption of neutral molecules minimizes both sample decomposition and ionization of the matrix material, thus simplifying the interpretation of mass spectra of mixtures. Here we use two-step laser desorption/laser ionization mass spectrometry, which consists of laser-induced desorption followed by laser ionization.[12-17] Laser-induced desorption has been shown to minimize decomposition.[12,16] A similar two-step instrument has been constructed by de Vries and Hunziker[18] which differs from ours in that the desorption laser wavelength is in the ultraviolet rather than the infrared region.

L^2MS Method. Our technique, two-step laser desorption/laser ionization mass spectrometry (L^2MS), has been described previously.[14,15,17] In the first step, shown in Figure 1, constituent molecules of the sample are desorbed with a pulsed infrared (IR) laser. The laser power is kept low to minimize decomposition. In the second step, the desorbed molecules are ionized with a pulsed ultraviolet (UV) laser and the resulting ions extracted into a reflectron time-of-flight mass spectrometer. In the particular ionization scheme presented here, 1 + 1 resonance-enhanced multiphoton ionization (1 + 1 REMPI), the UV laser is tuned to be in resonance with an excited state of the molecule of interest; absorption of a second photon then ionizes the molecule. Since the ionization efficiency of 1 + 1 REMPI exceeds that of nonresonant multiphoton ionization by orders of magnitude, the laser power can be chosen low enough so that only the molecules with a resonant state will be appreciably ionized. This simplifies the interpretation of mass spectra of complex mixtures. By tuning the wavelength of the ionization laser, we can select the class of compounds ionized. For the analysis of meteorite acid residues discussed here, we use an ionization wavelength of 266 nm, which ionizes polycyclic aromatic hydrocarbons (PAHs), a class of compounds found in extraterrestrial matter.[19-21]

As demonstrated previously, the key attributes of our instrument are (a) *in situ analysis*, minimizing the possibility of contamination and chemical alteration, (b) desorption with

† Present address: Laboratoire de Chimie Technique, EPFL, CH-1015 Lausanne, Switzerland.

0003-2700/92/0364-0682$03.00/0

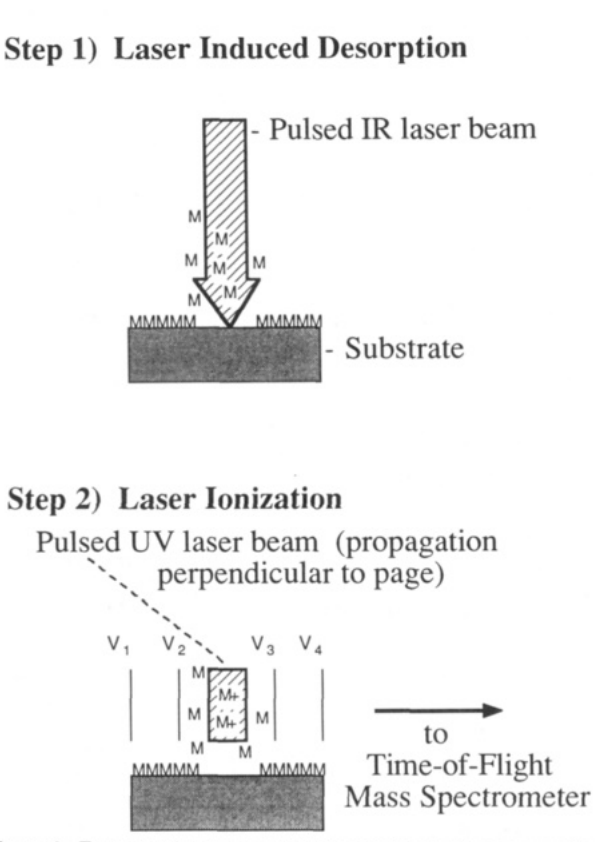

Figure 1. Two-step laser desorption/laser ionization mass spectrometry. In the first step, molecules (M) are desorbed intact from a substrate with a pulsed IR laser; in the second step, the desorbed molecules are ionized with a pulsed UV laser. These ions are then extracted into a time-of-flight mass spectrometer using a modified Wiley–McLaren geometry.

minimal decomposition and ionization with minimal fragmentation, resulting in spectra consisting primarily of *parent ion peaks* (although, fragmentation can be tuned in if desired by increasing the ionization laser power density), (c) *selective ionization* of only those molecules which have a transition in resonance with the UV laser photon energy, simplifying the spectra of complex mixtures, (d) high sensitivity with absolute detection limits in the *femtomole* range, (e) separation in time and space of the desorption and ionization steps, minimizing complex matrix effects found in single-step methods.

The ability of laser-induced desorption to volatilize neutral molecules intact, combined with the high sensitivity of laser ionization, makes two-step laser mass spectrometry a powerful technique for the organic analysis of particulates and inhomogeneous samples on a microscopic scale. We have recently modified our instrument, extending the spatial resolution from 1 mm to 40 μm. In this paper we demonstrate the extension of L^{2}MS to the organic analysis of particles 200 μm in diameter. In a later study,[22] we will demonstrate the application of this technique to a direct, in situ spatially-resolved analysis of the distribution of PAHs on a 40-μm scale for a freshly-cleaved sample of the Bishunpur meteorite.

Organic Analysis of Meteoritic Acid Residues. It has been shown that organic molecules are an indigenous constituent of carbonaceous chondrite meteorites;[19-21] classes of compounds include solvent-extractable aliphatic compounds, aromatic compounds, carboxylic and amino acids, and an acid-insoluble macromolecular material. The process by which these molecules were formed, however, remains a mystery. Possible synthetic mechanisms and source bodies include ion–molecule reactions in molecular clouds, Fischer–Tropsch–type and Miller–Urey syntheses in the solar nebula (the disk of gas and dust around the protosun or early Sun), and hydrolysis on the meteorite parent body.[23] Identification and characterization of these organic molecules can offer clues as to the process by which they were formed and thus provide insight into the origins and subsequent history of meteorites, ultimately leading to an understanding of conditions in the early solar system.

We describe here an investigation of the PAH composition of acid residues of interior samples of six different chondritic meteorites: the carbonaceous chondrites Murray (CM2) and Murchison (CM2), and the ordinary chondrites Bishunpur (L3.1), Semarkona (LL3.0), Saratov (L4), and Barwell (L6). All six were observed falls; so terrestrial contamination should be minimized. These meteorites are classified according to their primary and secondary characteristics:[24,25] the primary classification (CM, L, and LL shown here) is indicative of the original properties of the meteorite and is made on the basis of bulk chemistry and mineralogy, while the secondary classification, and petrographic type (e.g. 2, 3.0, 3.1, 4, and 6), is indicative of secondary processing the meteorite has undergone subsequent to its formation, such as aqueous alteration for types 1 and 2, or thermal metamorphism for types ≥3. Types 3.0 and 3.1 are transitional between aqueous alteration and thermal metamorphism. Semarkona (LL3.0) has undergone significant aqueous alteration,[26,27] while Bishunpur (L3.1) has undergone slight alteration and may have experienced some metamorphism.[27] The conventional explanation for the range of metamorphism seen in meteorites is that their grade reflects the depth of burial in their parent bodies (a parent body being the object in which a given meteorite or class of meteorites was originally located prior to separation). An L3 chondrite, for instance, probably came from the outer margins of the L-group parent body, while an L6 would have come from near the center. Estimates of the peak temperatures experienced by the ordinary chondrites are type 3 meteorites up to 870 K, type 4 meteorites 870–970 K, and type 6 meteorites 1020–1220 K.[28] The duration of time the meteorites spent at these temperatures is estimated to range from up to 10^6 years for type 3 to at least 10^7 years for type 6.[29] Aqueous alteration temperatures for CM2 chondrites are estimated to range from 270 to 290 K[30] and for Semarkona 270–520 K;[27] the durations remain unknown. We discuss the implications of this classification on our results in the Results and Discussion.

The meteorites in this study are known to contain only a small percentage (<2.8%) of carbon.[25] Therefore, to concentrate the organics, the meteorites were treated with acid which dissolves much of the mineral content.[31] PAHs are particularly robust with respect to acid treatment and thus do not undergo appreciable chemical alteration. Four of the residues analyzed here, Bishunpur, Semarkona, Saratov, and Barwell, were prepared by pulverizing samples of the meteorites and then subjecting these samples to a prolonged series of HCl and HF treatments (on the order of months) at room temperature. The residues were then washed with a small aliquot of water, with CS_2 to remove sulfur, and finally with acetone. The two residues of Murchison and Murray were prepared in a different manner; samples of these meteorites underwent a shorter duration of a similar acid treatment but the final HCl step was carried out at a higher temperature (60 °C). Table I shows concentration factors resulting from the acid treatments and the carbon content of the residues.[32]

Previous organic analyses of the Murchison meteorite include that by Hayes and Biemann[33] who investigated the organic constituents of meteorites, including Murray, by directly heating about 20–50 mg of a pulverized meteorite sample either at the entrance to a gas chromatograph–mass spectrometer or in the source region of a mass spectrometer. In studies by Orō[34] and by Pering and Ponnamperuma,[35] gram

Table I. Concentration Factor (Cf) as Well as the Percent Carbon for the Acid Residues Investigated

meteorite and type	specimen	Cf[a]	% C[b] (by weight)
Semarkona (LL3.0)[c]	USNM 1805	101	35.3
Bishunpur (L3.1)[c]	BM 1966,59	193	51.3
Murchison (CM2)[d]	BM 1970,6	37	
Murray (CM2)[d]	EKG 11.11.86	22	
Saratov (L4)[c]	BM 1956,169	175	2.4
Barwell (L6)[c]	BM 1966,59	144	1.2

[a] The concentration factor Cf is the inverse of the weight fraction remaining after residue preparation. [b] These values have been calculated from measured values for the bulk meteorite using Cf. [c] Acid residues prepared by John Arden, Oxford University. [d] Acid Residues prepared by Monica Grady, The Open University.

quantities of interior samples of the meteorite were first subject to analytical procedures to extract the soluble organic constituents, and then these extracts were analyzed with gas chromatography–mass spectrometry. Hayatsu et al.[36] have extensively investigated the composition of the insoluble macromolecular material by a variety of degradation techniques and have identified many of its constituent PAHs. More recently, Tingle et al.[37] analyzed in situ samples of meteorites, including Murchison, using a two-step method consisting of slow thermal desorption followed by laser ionization with vacuum ultraviolet light (118 nm); this technique required only 1–10 mg of sample. For comparison, they also used an ion-induced desorption method. de Vries et al.[38] have recently analyzed the vacuum sublimates of meteoritic acid residues using L^2MS combined with an intermediate jet-cooling step; their spectra show evidence of high masses.

We previously have demonstrated the application of L^2MS to the direct analysis of meteorites using the forerunner to the instrument described in this manuscript.[39,40] Our direct analysis of the Murray meteorite for its PAH constituents agrees well with the results of Hayes and Biemann, although the sensitivity of L^2MS was shown to exceed the former method. In a further study,[40] we analyzed the Allende meteorite for its spatial distribution of PAHs and found an inhomogeneous distribution on a 1-mm scale, the spatial resolution of our instrument at the time. What follows is a description of the newest instrument modifications enabling microscopic organic analysis on a 40-μm scale and the results of an analysis of six meteoritic acid residues.

EXPERIMENTAL SECTION

Instrument Modifications. A schematic of our microanalytical instrument is shown in Figure 2. This instrument differs from a previous version[39,40] by the incorporation of a microscope objective, rather than a lens, into the vacuum chamber to focus more tightly the IR desorption laser beam onto the sample. We chose an objective composed of Cassegrainian optics because of two advantages these have over conventional optics: they provide a larger working distance and are achromatic. Even with the larger working distance, optimization of the ion collection efficiency required extensive modification of the extraction region because the objective distorts the extraction field lines. Aided by computer simulations of ion trajectories in the extraction region using the program SIMION (David Dahl, EG&G, Idaho National Engineering Lab, Idaho Falls, Idaho), we found that the field distortion could be minimized by floating the objective. The achromaticity of the Cassegrainian optics is needed so that the focal point of the infrared desorption laser beam coincides with that of the visible light used to observe and position the sample. To obtain sensitive control over the position of the sample with respect to the microscope objective (and thus with respect to the desorption laser beam focus), we added an x–y–z manipulator; to enhance sample viewing, we added a video camera system.

Procedure. The sample to be analyzed is attached to a nonconducting platter, either glass or a machinable ceramic, Macor

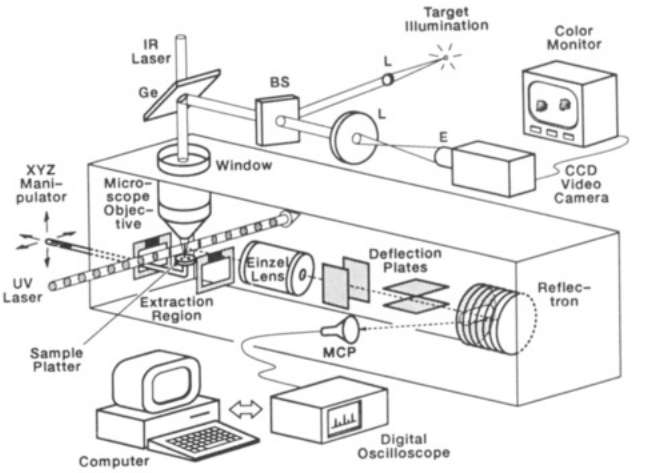

Figure 2. Schematic of microanalytical instrument. Some abbreviations are L = lens, E = apertured eyepiece, BS = beam splitter, MCP = microchannel plate, and Ge = germanium flat which reflects visible light but transmitts IR light. Only the outer two of four extraction electrodes are shown (see Figure 1 for a side view of the extraction region).

(Corning Glass Works, Corning, NY), and is introduced into the chamber through a vacuum interlock which is pumped down to 1×10^{-3} Torr in about 2 min. After introduction into the main chamber, samples are left to outgas for about 15 min until the pressure in the main chamber returns to the original base pressure of less than 5×10^{-8} Torr.

The sample platter is positioned just below the extraction region and brought into focus using an x–y–z manipulator. For sample viewing, an aperturing eyepiece and field lens are used in a telescope mode, so that an image of the sample is projected onto a CCD video camera. The incorporation of an aperturing microscope eyepiece, rather than a standard unapertured eyepiece, greatly increases the clarity of the image by removing stray light. To couple the video camera to the microscope objective, a germanium flat is used which reflects visible light but transmitts the infrared light of the desorption laser. The sample is illuminated with a quartz halogen lamp which is incident either at an angle normal to the surface of the platter or at a glancing angle. In the former method, as shown in Figure 2, the light passes through the objective; in the latter, the light is focused loosely with a lens external to the chamber and is introduced through a side viewport (not shown in the figure).

Infrared light from a pulsed CO_2 laser (Alltec AL 853; 10.6 μm, 120-ns fwhm with a 4-μs tail) is attenuated with a series of germanium flats, collimated with an iris to the diameter of the microscope entrance mirror, 5 mm, and then focused with the reflecting microscope objective (Ealing ×36) to a 40-μm diameter spot on the sample. The laser pulse energy is chosen to maximize the desorption yield without producing fragmentation or ionization. A typical pulse energy is measured to be 22 μJ; we estimate 5.2 μJ is contained in the initial spike, and 16.8 μJ in the tail. (The pulse shape depends on the CO_2 laser gas mixture. In these experiments we use a gas mixture containing 18% N_2, which provides the most stable operation: shot-to-shot fluctuations in the peak intensity of the laser profile are less than 10%. Removal of the N_2 from the gas mixture eliminates the 4-μs tail but results in a much less stable operation.) From these measurements the IR laser power density is estimated to be 2.8×10^6 W/cm^2.

After an appropriate time delay (19 μs), the fourth harmonic of a pulsed Nd:YAG laser (Spectra Physics DCR11; 266 nm, 8-ns fwhm) is attenuated with a polarizer and then focused with a cylindrical lens (25-cm focal length) into a ribbon which passes between the extraction electrodes where the laser beam selectively ionizes desorbed molecules that have a transition in resonance with the laser wavelength, in this case PAHs. The ionization laser pulse energy is chosen to maximize parent ion signal intensities produced by 1 + 1 REMPI with minimal fragmentation; a typical pulse energy is 520 μJ. We estimate the UV laser power density to be 5.4×10^6 W/cm^2.

A pulse generator with an adjustable delay is used to trigger both lasers. The Nd:YAG laser is triggered at its optimal rate,

10 Hz. Since we want to take single desorption shots, the trigger pulses for the CO_2 laser first pass through a homemade pulse–repressor box which allows the trigger to continue to the CO_2 laser only after a pushbutton has been activated. The Nd:YAG trigger pulses serve as a clock so that the CO_2 laser pulse arrives 19 μs ahead of the Nd:YAG laser pulse.

The ions produced by the UV laser are extracted from the source using a modified Wiley–McLaren geometry.[41] This accomplishes longitudinal space focusing of the ions in a field-free region outside the source. The tightest focus is achieved by keeping the focal length as short as possible, because the faster the ion pulse can be brought to a focus the less time it has to broaden due to the nascent ion kinetic energy spread. In reality, it is impracticable to place the detector so close to the source since this will result in unreasonably short flight times and, consequently, low mass resolution due to poor temporal separation between ions of differing masses. By combination of Wiley–McLaren and reflectron geometries, this difficulty can be overcome. In our system the ions are focused close to the source and are then allowed to spread along the length of the flight tube. The reflectron, acting as an ion mirror,[42] turns the ions about such that the spreading ion pulse is refocused back to a secondary space focus centered on the detector and in the same plane as the primary focus. This greatly improves mass resolution by lengthening the flight time while maintaining the narrow width of the ion pulse obtained at the primary focus.

Ion collection efficiency is maximized by transverse focusing with an Einzel lens after extraction and by the use of two sets of defection plates to steer the ions to the detector. The total flight path is 3 m. A dual microchannel plate (Galileo TOF-2003) is used in a Chevron configuration to detect the ions; the output passes through a fast preamplifier and a timing filter and is displayed on a 125-MHz digital oscilloscope. The spectra shown here consist of an average of 15 shots. For data processing and storage, the oscilloscope is interfaced to a computer.

As an internal reference, a leak value is used to introduce a constant supply of toluene ($C_6H_5CH_3$) as a reference gas. This enables periodic optimization of the ion collection optics.

Instrument Characterization. The mass scale was calibrated using two known compounds, toluene (92.06 amu) and coronene (300.09 amu). For the mass spectra presented here, the mass resolution ($m/\Delta m$) is 490, where m is the mass and Δm is the fwhm. Subsequent to these experiments, we have increased the mass resolution to over 1000 by replacing some warped plates in the reflectron with more rigid ones.

The spatial resolution of our instrument is determined by the diameter of the desorption laser spot. To measure the diameter of this spot, a sample platter was coated with a red dye (Texas Red). The diameter of the bare spot produced by a single desorption laser shot is measured to be at most 40 μm.

To measure the sensitivity of the instrument, we prepared samples of a nonvolatile adsorbate, coronene ($C_{24}H_{12}$), of various thicknesses, on a smooth Macor substrate. The samples were prepared by applying a fixed aliquot of a known solution of coronene in toluene onto a ceramic dish and then letting the toluene evaporate; the thickness of the coronene layer was varied by varying the concentration of the coronene solution. From the known amount of coronene applied and the diameter of the desorption laser spot, the sensitivity of our instrument is estimated to be 8 fmol (4.8×10^9 molecules) of coronene exposed to the desorption laser. (Subsequent to this measurement, we discovered that the residue of coronene left after the evaporation of the solvent is not uniformly distributed over the drop area; rather, it is concentrated along the rim of the spot. Therefore we expect the detection limit of our instrument to be even smaller. Measurements are underway using a vapor deposition method to produce a more uniform layer of coronene.) This sensitivity is comparable to that of the previous version of our instrument.[40] However, since the desorption laser spot is now so much smaller (40 μm rather than 1 mm), the minimum detectable sample concentration must be greater. The detection limit of our new instrument in ppm is therefore poorer than the previous instrument by a factor of 625 (the ratio of the spot areas).

Sample Handling and Manipulation. The meteoritic acid residues analyzed here consists of particles 200 μm in diameter and were supplied in glass vials. To ensure safe transfer of these particles into the vacuum chamber, we attach them to the sample platter with a thermoplastic polymer, Crystalbond (Armeco Products, Inc. Ossening, NY), which does not give any interfering signals in the mass spectrum. We constructed a heating stage on a second microscope (independent from our instrument) to melt microscopic grains of Crystalbond on the sample platter at a temperature no greater than 90 °C. The particle of interest is then transferred to the platter with a clean stainless steel needle; it is removed from the needle when it comes in contact with the melted Crystalbond. Care is taken to keep the grains of adhesive much smaller than the particles themselves so that the latter do not become occluded. Upon cooling, the Crystalbond solidifies and the particle is thus attached to the platter, as shown in Figure 3.

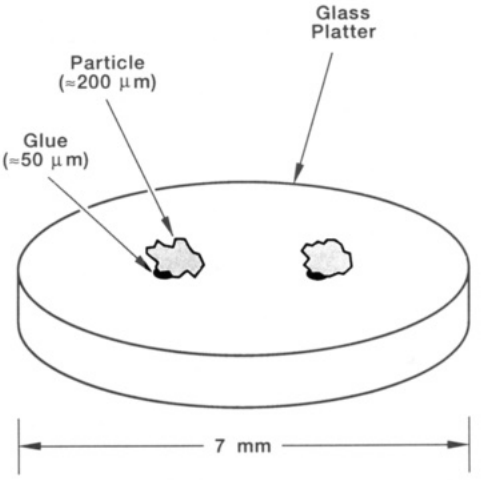

Figure 3. Schematic of particles mounted on the sample platter.

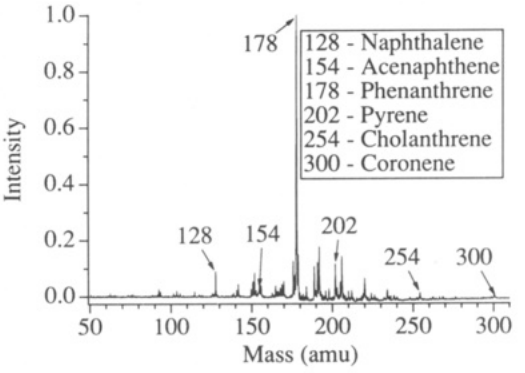

Figure 4. Mass spectrum of the Bishunpur (L3.1) acid residue. The spectrum is a 15-shot average. Peaks corresponding to masses of bare PAH skeletons are indicated.

RESULTS AND DISCUSSION

Mass Spectra of Acid Residues. We analyzed six acid residues from meteorites for their PAH content using L^2MS. These samples were obtained in submilligram quantities, too little for analysis with our previous instrument.[40] Since evidence indicates the ordinary chondrite Bishunpur (L3.1) to have undergone the least processing after accretion, the organics it contains are expected to be the closest to the original starting material. A mass spectrum of the Bishunpur acid residue is shown in Figure 4. The spectrum consists of a 15-shot average. The sample was repositioned between laser shots so that desorption occurred each time from a fresh portion of the sample; in this particular case, a total of three particles, each about 200 μm in diameter, were analyzed to obtain the spectrum. No peaks were detected at masses greater than 300 amu; peaks at masses less than 100 amu were less than 2% of the maximum peak intensity and most likely originated from fragmentation.

To obtain possible mass assignments, we first identify masses that correspond to those of bare PAH skeletons; peaks

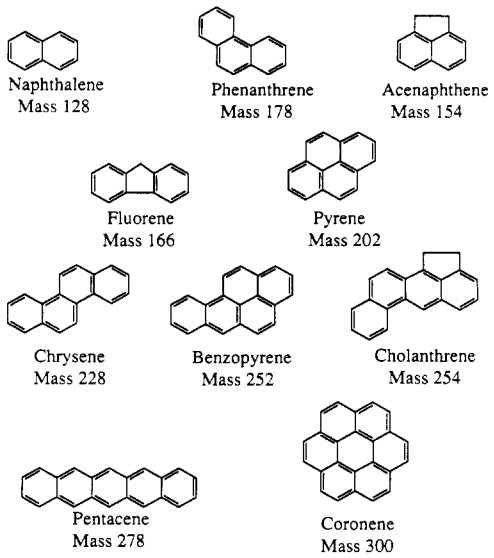

Figure 5. Some PAH skeletons and their masses in amu.

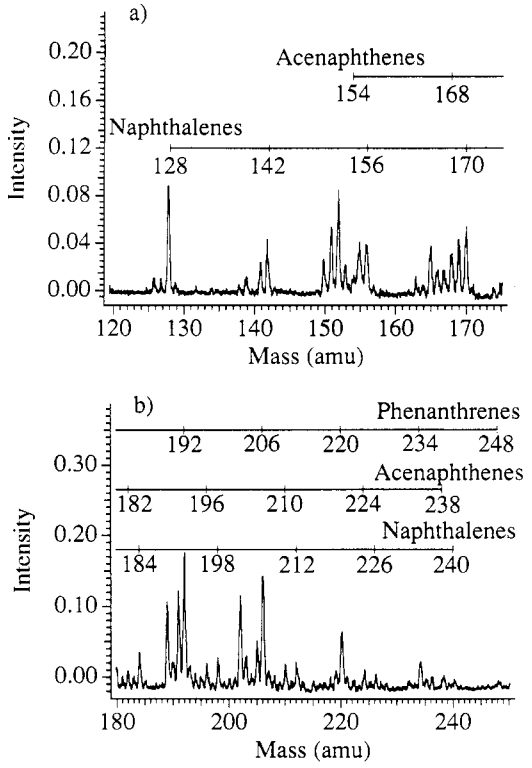

Figure 6. Expansion of the Bishunpur spectrum (a) for masses less than 178 amu and (b) for masses greater than 178 amu. Series of masses corresponding to successively alkylated PAHs are indicated; however, we cannot distinguish between possible isomers.

at these masses are indicated in Figure 4. Some possible structures of these molecules are shown in Figure 5; we are not able to distinguish between isomers without changing the ionization laser wavelength. We then identify series of peaks with characteristic increments of 14 amu, indicative of successively alkylated PAHs in which –H is replaced by $-CH_3$. Three such series are clearly observed in an expansion of the Bishunpur mass spectrum, shown in Figure 6, suggesting the presence of extensively alkylated PAHs. A list of possible mass assignments is given in Table II. There are also many peaks for which we have neglected to give possible assignments. Some of the peaks which occur at odd mass units may correspond to the ^{13}C-containing isotopic homologues of the molecules listed in Table II. There is also the possibility of contributions due to fragmentation, an example of which is

Table II. Possible Peak Assignments for Two-Step Laser Mass Spectrum of Bishunpur Acid-Insoluble Residue

mass, amu	possible assgnt (isomers not listed)[a]	molecular formula
128	naphthalene	$C_{10}H_8$
142	C_{11}-alkyl-naphthalene	$C_{11}H_{10}$
152	fragment of mass 178 (verified)	$C_{12}H_8$
154	acenaphthalene	$C_{12}H_{10}$
156	C_{12}-alkyl-naphthalene	$C_{12}H_{12}$
166	fluorene	$C_{13}H_{10}$
168	C_{13}-alkyl-acenaphthene	$C_{13}H_{12}$
170	C_{13}-alkyl-naphthalene	$C_{13}H_{14}$
178	phenanthrene	$C_{14}H_{10}$
182	C_{14}-alkyl-acenaphthene	$C_{14}H_{14}$
184	C_{14}-alkyl-naphthalene	$C_{14}H_{16}$
192	C_{15}-alkyl-phenanthrene	$C_{15}H_{18}$
196	C_{15}-alkyl-acenaphthene	$C_{15}H_{16}$
198	C_{15}-alkyl-naphthalene	$C_{15}H_{18}$
202	pyrene	$C_{16}H_{10}$
206	C_{16}-alkyl-phenanthrene	$C_{16}H_{14}$
210	C_{16}-alkyl-acenaphthene	$C_{16}H_{18}$
212	C_{16}-alkyl-naphthalene	$C_{16}H_{20}$
220	C_{17}-alkyl-phenanthrene	$C_{17}H_{22}$
224	C_{17}-alkyl-acenaphthene	$C_{17}H_{20}$
226	C_{17}-alkyl-naphthalene	$C_{17}H_{22}$
228	chrysene	$C_{18}H_{12}$
234	C_{18}-alkyl-phenanthrene	$C_{18}H_{18}$
238	C_{18}-alkyl-acenaphthene	$C_{18}H_{22}$
240	C_{18}-alkyl-naphthalene	$C_{18}H_{24}$
248	C_{19}-alkyl-phenanthrene	$C_{19}H_{20}$
252	C_{19}-alkyl-acenaphthene	$C_{19}H_{24}$
252	benzopyrene	$C_{20}H_{12}$
254	cholanthrene	$C_{20}H_{14}$
254	C_{19}-alkyl-naphthalene	$C_{19}H_{26}$
266	C_{20}-alkyl-acenaphthene	$C_{20}H_{26}$
266	C_{21}-alkyl-benzopyrene	$C_{21}H_{16}$
268	C_{20}-alkyl-naphthalene	$C_{20}H_{28}$
276	C_{21}-alkyl-phenanthrene	$C_{21}H_{16}$
278	pentacene	$C_{22}H_{14}$
280	C_{21}-alkyl-acenaphthene	$C_{21}H_{28}$
280	C_{22}-alkyl-benzopyrene	$C_{22}H_{16}$
292	C_{22}-alkyl-pentacene	$C_{23}H_{16}$
294	C_{22}-alkyl-acenaphthene	$C_{22}H_{30}$
294	C_{23}-alkyl-benzopyrene	$C_{23}H_{18}$
300	coronene	$C_{24}H_{12}$

[a] The notation C_n-alkyl-X denotes that the peak is assigned to molecules containing n carbon atoms arranged as the isomers of the alkylated X compound.

the peak at 152 amu, which we have seen corresponds to the mass of a fragment of phenanthrene. Finally, heteroatom PAH species where, for example, a –CH is replaced by –N, may be present. We chose, however, to list only PAHs in Table II because REMPI at 266 nm is known to be a highly sensitive detection technique for these molecules.

A word of warning in relating peak intensities to concentrations of the compound in the sample: when 1 + 1 REMPI is used as the ionization technique, parent ion peak intensities are not only proportional to the concentration of the compound in the sample but also depend on the absorption cross section of that compound at the ionization laser wavelength. Relative absorption cross sections for several PAHs are given in ref 39.

Mass spectra of five other acid residue samples, run under similar experimental conditions, are shown in Figures 7 through 9. Intensity scaling relative to Bishunpur is indicated in the lower right-hand corner of each spectrum. One striking similarity evident in all these acid residue spectra is that the highest intensity peak occurs at mass 178 amu; however, the absolute intensity of that peak is very different for different meteorites. A background spectrum, obtained with the desorption laser focused on a bare spot of the sample platter, is shown in Figure 7b.

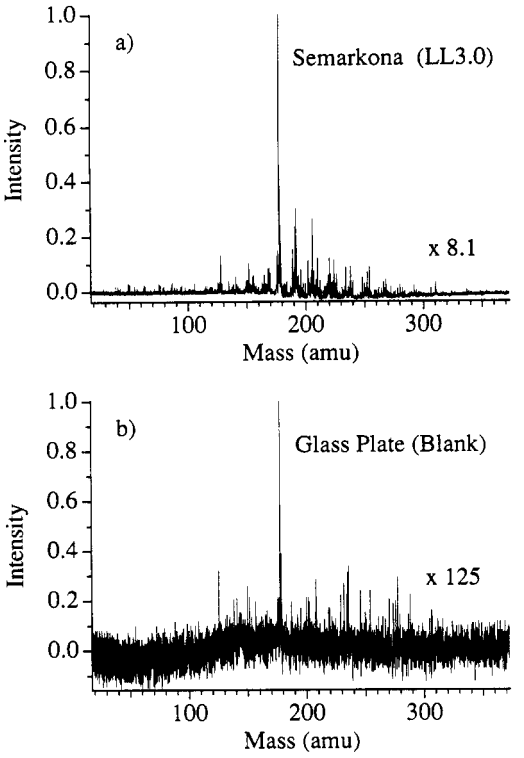

Figure 7. (a) Mass spectrum of the Semarkona (LL3.0) acid residue. (b) Background mass spectrum of the glass sample platter. Relative intensity scalings with respect to the Bishunpur spectrum shown in Figure 4 are indicated in the lower right-hand corners.

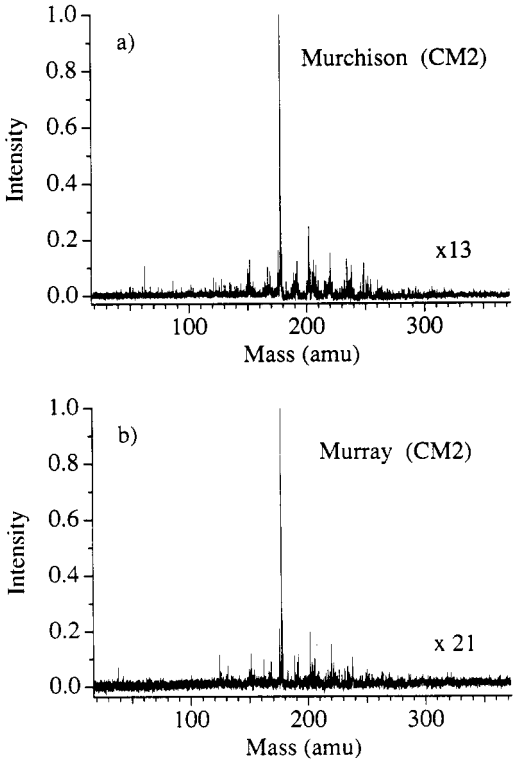

Figure 8. Mass spectra of the (a) Murchison (CM2) and (b) Murray (CM2) acid residues. Relative intensity scalings with respect to the Bishunpur spectrum shown in Figure 4 are indicated in the lower right-hand corners.

Both the Bishunpur (L3.1) and Semarkona (LL3.0) meteorites are "unequilibrated ordinary chondrites", which are known to contain small amounts of carbon, about 0.1–1.1%.[25] The type 3 petrographic classification indicates that they have

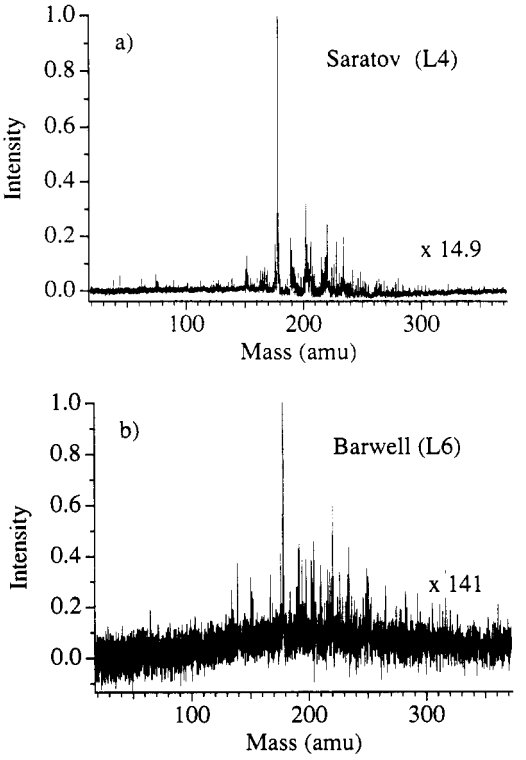

Figure 9. Mass spectra of the (a) Saratov (L4) and (b) Barwell (L6) acid residues. Relative intensity scalings with respect to the Bishunpur spectrum shown in Figure 4 are indicated in the lower right-hand corners.

undergone the least metamorphism, though the final classification into 3.1 and 3.0 indicates evidence of some aqueous alteration, a change in mineralogy caused by chemical reactions between solids and fluids. Bishunpur (L3.1) is believed to be among the most primitive matter in the solar system in that it has undergone the least secondary processing, while Semarkona (3.0) has undergone slightly more aqueous alteration. Their spectra, shown in Figures 4 and 7a, indicate that they contain substantial amounts of PAHs.

The Murchison (CM2) and Murray (CM2) meteorites are "carbonaceous chondrites", classified as such because they contain relatively high concentrations of carbon, about 1.5–2.8%.[25] The type 2 petrographic classification indicates that they have undergone considerable aqueous alteration. Their spectra, shown in Figure 8, qualitatively agree with previous analyses made of crushed meteorite samples that did not undergo the acid treatment;[39] however, the relative peak heights within a spectrum differ somewhat from those of crushed samples. This may be caused by inhomogeneities within the meteorites themselves, or by differences in desorption laser powers, or by the differing sample preparation techniques. Moreover, we observe that the relative heights of low- and high-mass peaks within a spectrum depend on the desorption laser power: as the laser power increases, the peak heights at lower masses (<128 amu) increase with respect to those at higher masses. We have observed similar behavior for charcoal samples spiked with various known PAHs, and for spiked zeolites as well, indicating that these lower mass peaks are fragments; we have not observed this behavior with pure compounds desorbed from nonporous substrates, such as Macor.[43] This suggests that the mechanism of desorption differs for porous and nonporous substrates. Perhaps molecules adsorbed on a porous matrix do not escape as readily, and so desorb with more internal energy than those adsorbed on a nonporous substrate, and thus tend to fragment. In practice, we keep the desorption laser power as low as possible so as to minimize fragmentation. Even so, the Murchison

spectrum contains substantial low-mass peaks, not shown in the figure.

The Saratov (L4) and Barwell (L6) meteorites are "equilibrated ordinary chondrites", which contain less than 0.2% carbon.[25] The spectra of their acid residues are shown in Figure 9. The type 4 petrographic classification indicates that the Saratov meteorite has undergone significant thermal metamorphism. Nevertheless, our analysis indicates that PAHs are present. This conclusion corroborates the recent results of a study done in collaboration with Marti and coworkers[44] that indigenous organic matter is present in some equilibrated ordinary chondrites; in that study we found the Forest Vale (H4) meteorite to contain PAHs.

The type 6 petrographic classification of Barwell indicates that this meteorite has undergone the highest degree of thermal metamorphism. The absence of PAHs in this sample at the limit of our sensitivity, its spectrum being indistinguishable from the background spectrum (Figure 7b), is reasonable considering its petrographic classification.

Contamination Studies. One of our primary concerns is terrestrial contamination. Potential sources of contamination in our laboratory fall into four categories: sample-handling tools, laboratory air, virtual leaks (sources of PAHs inside the vacuum chamber), and redeposition of laser-desorbed material from one particle onto a neighboring one. To minimize the contamination introduced during sample preparation, all manipulation is done quickly with stainless steel tools, which have been rinsed in methanol and ultrasonicated; gloves are worn throughout the process. Typical exposure times to laboratory air are 15 min.

To quantify the contamination introduced from exposure to laboratory air, we used acid residues themselves as controls. One of the samples, Barwell, proved to give very weak PAH signals, as shown in Figure 9b. After exposure of this sample to laboratory air for over 24 h, no increase is observed in the PAH signal intensities. Since the contamination signal intensity can depend on the physical characteristics of the individual sample (for example, a porous material will likely give a larger contamination signal than a nonporous one), we also exposed the acid residue with the largest PAH signals, Bishunpur, to the laboratory air, this time for 4 days. Again, we saw no discernible change in the mass spectrum.

To test for contamination from virtual leaks of PAHs inside our vacuum chamber, we exposed the Barwell and Bishunpur samples to the chamber for 2 h; again, the signals did not change. Finally, to test for contamination by redeposition, a sample platter was prepared with particles of both Barwell and Bishunpur, separated by 200 μm. We compared mass spectra of the Barwell particles taken before and after analysis of the Bishunpur particles; no difference in signal intensities could be detected.

We conclude that the contamination of these acid residue samples from our sample handling and analysis technique is probably less than the background signal intensity shown in Figure 7b, although there remains the possibility of contamination introduced prior to our receiving the samples. Of course we cannot rule out that some source of contamination contributes to our observations, but the different mass spectra observed for the acid residues of different meteorites argues persuasively that any contamination is not from a common source.

Comparison between Meteorites. To simplify qualitative comparison between meteorites, bar graphs of peak intensities of selected masses are plotted in Figure 10. Selected masses correspond to those of bare PAH skeletons (excluding the peak at 178 amu whose mass corresponds to that of phenanthrene), alkylated phenanthrenes (colored in black), and an alkylated naphthalene whose peak is of appreciable size. The intensities

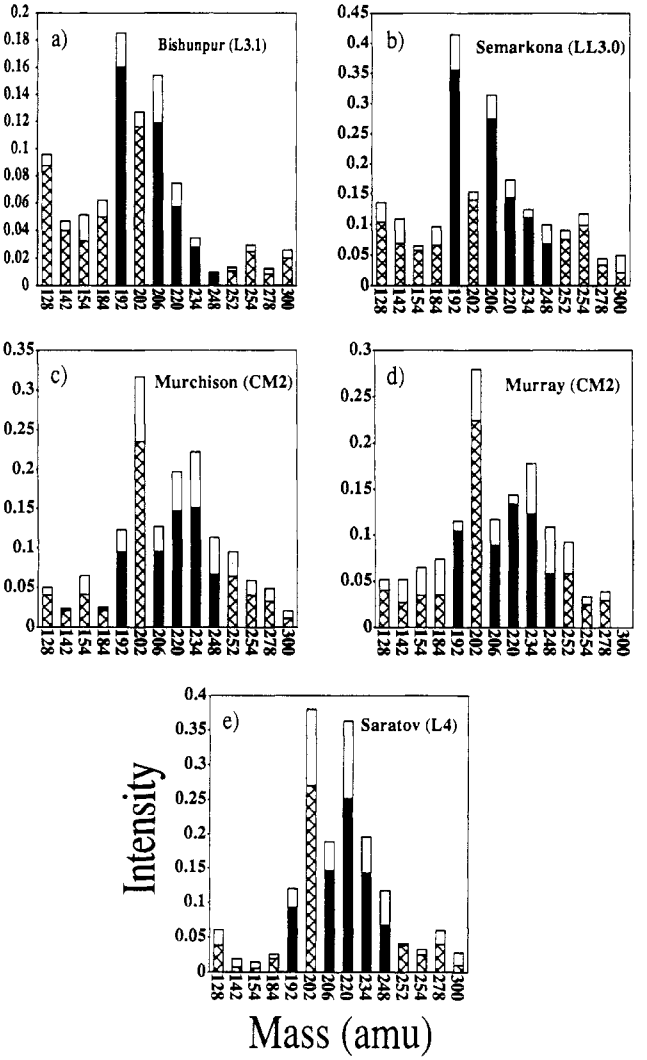

Figure 10. Bar graphs of selected mass peaks for the meteoritic acid residues. Intensities are plotted with respect to the peak intensity at 178 amu. The top, unshaded portion of each bar represents plus one standard deviation. Masses corresponding to the alkylated phenanthrene series are shaded black.

are relative to the mass 178 amu peak intensity. Each bar graph represents an average of three spectra. The standard deviation, σ, of the data is indicated by the white rectangles above each bar; only "$+\sigma$" is displayed.

One striking difference between meteorites is the relative intensities of the 192 and 202 amu peaks. For the unequilibrated ordinary chondrites (Figure 10a,b), and 192 amu peak dominates the 202 amu peak, while the reverse is seen for the carbonaceous chondrites (Figure 10c,d) and for the equilibrated ordinary chondrite Saratov (Figure 10e).

Another noticeable difference is seen in the series of alkylated phenanthrenes (colored in black). The unequilibrated ordinary chondrites show a steady decrease in intensity with increasing alkylated-phenanthrene mass, Bishunpur more rapidly than Semarkona. In contrast, the carbonaceous chondrites and the ordinary chondrite Saratov exhibit an increase at 220 and 234 amu, indicating more extensive alkylation of the phenanthrene skeleton.

The organic material in acid residues is believed to be macromolecular in nature, similar to terrestrial kerogen,[45] which consists principally of large, randomly oriented, polycyclic aromatic sheets.[46] Therefore it is surprising that we have not found evidence of molecules with masses significantly greater than 300 amu. However, Hayatsu et al.[36,47,48] have proposed that the basic building blocks of macromolecular

material are small aromatic ring structures with up to only four rings, that are linked by short methylene chains, esters, sulfides, and biphenyl groups. We have evidence for up to five- and six-ring structures with extensive alkylation, but with our present setup we cannot distinguish the presence of nitrogen, oxygen, and sulfur components. Our results support the suggestion of Hayatsu et al.[48] that the building blocks may be relatively small molecules.

An alternative explanation for the absence of high-mass peaks in our spectra might be that our detection sensitivity is poor for these large aromatic hydrocarbons. Recall that signal intensity depends on the absorption cross section of the individual compound is the ionization laser wavelength. UV spectra of PAHs indicate a general trend for the absorption maximum to shift to longer wavelengths as the number of aromatic rings in conjugation increases. For the case of a fixed ionization wavelength of 266 nm, the absorption cross section is greatest for moderate-mass PAHs, such as phenanthrene. Thus, it might be possible to increase the detection sensitivity for high-mass PAHs by tuning the ionization wavelength to the red using the output of a frequency-doubled YAG-pumped dye laser. Since we have a suitable dye laser available, we shall soon attempt to test this hypothesis.

An interesting question is whether organics in the different chondrites originated from different sources or had a common origin, as would be expected if the organics formed either in the interstellar dust cloud prior to formation of the solar nebula or in the solar nebula prior to meteorite parent body formation. It is useful to digress here to outline some present thoughts[20] concerning the origin of organics. The protosolar nebula, before gravitational instability initiated the generation of the solar system, is believed to have been very cold (below 50 K) and to have contained a rich diversity of complex molecules, dust particles, and interstellar grains formed in numerous stellar environments. If such material were to have survived the formation of the solar system, then we might expect to see large isotopic variations in the matter that surrounds us. Yet isotope analysis carried out on samples from the Earth, meteorites, the moon, and Mars has shown, on the whole, how isotopically uniform is the matter in our solar system. It has also been noted that there is a chemical gradation (increasing volatile content) of the planets as their distances increase from the Sun.[49] To explain both these observations, it has been suggested that early on in the evolution of the solar nebula there was a dramatic increase in temperature of up to 2000 K[50] as accretion occurred. At such temperatures and anticipated pressures of 10^{-6}–10^{-2} atm, all matter would have been vaporized. As a result, the nebula would have achieved a state of chemical and isotopic homogeneity from which organics could subsequently form, when the nebula cooled. This is the so-called "condensation model". Subsequent formation of meteorite parent bodies and the planets at various nebular temperatures (when some elements were still in the gas phase) and/or fractionation of dust from the gas, could in principle, explain the different compositions of the meteorites and planets. This model is at best a gross oversimplification and, in fact, micrometer-sized presolar grains of diamond, graphite, and silicon carbide have been found, albeit in trace amounts, in members of all the chondrite classes.[51] Nevertheless, the condensation model remains the framework around which our current understanding of the early evolution of the solar system is based.

The ordinary chondrite parent bodies are thought, on the basis of meteorite mineralogy and volatile trace element abundances, to have formed when the nebula had cooled to about 450–500 K.[19] Organic synthesis, at least by the Fischer–Tropsch mechanisms, requires catalysts that would not be thermodynamically stable until temperatures had dropped below 400 K.[19] Thus, the condensation model predicts that ordinary chondrites ought not to contain any organics! Our results clearly are in conflict with this prediction, which makes the detection of organics in ordinary chondrites of special interest.

We see variations in the distribution of PAHs for different meteorite classes. Assuming a common origin of organics, the variations from meteorite to meteorite could be explained in terms of secondary (postaccretional) processing. Ordinary chondrites are believed to be fragments of larger parent bodies. It is generally accepted that there were at least three parent bodies, each corresponding to a different primary classification of ordinary chondrite, H, L, and LL.[52] The degree of thermal metamorphism, as indicated by the meteorite's petrographic type 3, 4, etc., reflects both the temperature and duration of heating experienced by the meteorite. The most popular model of metamorphism is that the ordinary chondrite parent bodies were internally heated after their accretion by radioactive decay of ^{26}Al. Clearly, those portions of the parent bodies closest to the center (types 5–6) would have experienced higher temperatures for longer periods than those nearer the edge (types 3–4). This gives rise to the so-called "onion shell" model of parent bodies.[53]

Thermal metamorphism ought to result in graphitization of the macromolecular material by a process similar to that of coalification.[54] In general, however, it is observed that the more metamorphosed ordinary chondrites, types 3.6–6, contain little or no graphite.[55,56] So either the original organics were completely destroyed during thermal metamorphism by a process such as oxidation by iron oxides[57] or the material from which ordinary chondrites of petrographic types 3.6–6 formed never contained any organics. This latter hypothesis is compatible with a modified version of the condensation model in which the nebula might have been cooling sufficiently during the formation of ordinary chondrite parent bodies so that by the time the outer layers of these bodies had accreted, the nebula temperature was low enough for organics to form. Analysis of meteorites of petrographic types 3.4–4 (intermediate metamorphism) may help distinguish between these scenarios. Our observation of the presence of organics in Saratov (L4) is significant, but some caution is required. Because aromatics are more stable to thermal decomposition and oxidation than aliphatics, metamorphic processing should promote greater aromaticity. Hence, we expect the ratio of aromatics to aliphatics to grow with increasing petrographic type if organics in meteorites have a common origin that predated the formation of their parent bodies. The phenanthrenes of Saratov are seen to be more alkylated than those of Bishunpur and Semarkona, not what is to be expected if Saratov underwent more thermal metamorphism. Because Saratov was the only L4 residue we analyzed, the possibility of terrestrial contamination cannot be ruled out. In light of this, we plan to analyze more residues of this type to establish the validity of this result.

As for the carbonaceous chondrites, aqueous alteration may have significantly affected their macromolecular material. For instance, Shock and Schulte[58] have suggested that amino acids and other water-soluble organic compounds found in CM2 chondrites were formed by aqueous alteration of the macromolecular material. If alkylated products are intermediates in this process, then the greater alkylation observed by us in the CM2s, Murchison and Murray, is consistent with this interpretation. A similar process might also explain the greater alkylation of Semarkona over Bishunpur.

The mechanisms responsible for the modification of the macromolecular material during thermal metamorphism and aqueous alteration are likely to be complex and not easily deduced theoretically. Experimental attempts to mimic these

two processes will be essential in the interpretation of studies of the organic material in meteorites. The experiments must be carried out on meteorites that have undergone the least secondary processing, such as Bishunpur. Analysis of terrestrial analogues, for which there is more material, may also prove useful, particularly if reaction kinetics are slow.

In summary, we have identified significant trends in the PAH composition of several meteorites, thus enabling us to distinguish between different classes and type of meteorite on the basis of their trace organic compounds.

ACKNOWLEDGMENT

We are indebted to John W. Arden, Department of Earth Sciences, Oxford University, Oxford, U.K., and Monica M. Grady, Department of Earth Sciences, The Open University, Milton Keynes, U.K., who prepared the acid residues and kindly made them available to us. In addition, we thank M. S. de Vries and H. E. Hunziker, IBM Research Division, Almaden Research Center, San Jose, CA, for useful discussions. We gratefully acknowledge the support of the IBM Corp, NASA (Grant NAG 9-458), and the Stanford Office of Technical Licensing. In addition, C.R.M. thanks the National Science Foundation for a graduate fellowship and J.-M.P. thanks the Swiss National Science Foundation for a postdoctoral fellowship.

REFERENCES

(1) *Secondary Ion Mass Spectrometry SIMS V*; Benninghoven, A., Colton, R. J., Simons, D. S., Werner, H. W., Eds.; Springer Series in Chemical Physics 44; Springer-Verlag: Berlin, 1986.
(2) Benninghoven, A.; Sichtermann, W. K. *Anal. Chem.* **1978**, *50*, 1180–1184.
(3) Cotter, R. J. *Anal. Chim. Acta* **1987**, *195*, 45–59.
(4) Posthumus, M. A.; Kistemaker, P. G.; Meuzelaar, H. L. C.; TenNoever de Brauw, M. C. *Anal. Chem.* **1978**, *50*, 985–991.
(5) Briggs, D. *SIA, Surf. Interface Anal.* **1983**, *5*, 113–118.
(6) Gillen, G.; Simons, D. S.; Williams, P. *Anal. Chem.* **1990**, *62*, 2122–2130.
(7) Novak, F. P.; Wilk, Z. A.; Hercules, D. M. *J. Trace Microprobe Tech.* **1985**, *3*, 149–163.
(8) Wilk, Z. A.; Hercules, D. H. *Anal. Chem.* **1987**, *59*, 1819–1825.
(9) Kimock, F. M.; Baxter, J. P.; Winograd, N. *Nucl. Instrum. Methods Phys. Res.* **1983**, *218*, 287–292.
(10) Conzemius, R. J.; Capellan, J. M. *Int. J. Mass Spectrom. Ion Phys.* **1980**, *34*, 197–271.
(11) Williams, P.; Sundqvist, B. *Phys. Rev. Lett.* **1987**, *58*, 1031–1034.
(12) Grotemeyer, J.; Boesl, U.; Walter, K.; Schlag, E. W. *Org. Mass. Spectrom.* **1986**, *21*, 595–597, 645–653.
(13) Tembreull, R.; Lubman, D. M. *Anal. Chem.* **1987**, *59*, 1003–1006.
(14) Engelke, F.; Hahn, J. H.; Henke, W.; Zare, R. N. *Anal. Chem.* **1987**, *59*, 909–912.
(15) Hahn, J. H.; Zenobi, R.; Zare, R. N. *J. Am. Chem. Soc.* **1987**, *109*, 2842–2843.
(16) Li, L.; Lubman, D. M. *Rev. Sci. Instrum.* **1988**, *59*, 557–561.
(17) Hahn, J. H.; Zenobi, R.; Zare, R. N. *Bull. Chem. Soc. Jpn.* **1988**, *61*, 87–92.
(18) de Vries, M. S.; Elloway, D. J.; Wendt, H. R.; Hunziker, H. E. Submitted for publication in *Rev. Sci. Instrum.*
(19) Hayatsu, R.; Anders, E. *Topics in Current Chemistry*; Springer-Verlag: Berlin, 1981; Vol. 99, pp 1–37.
(20) Mullie, F.; Reisse, J. *Topics in Current Chemistry*; Springer-Verlag: Berlin, 1987; Vol. 139, pp 85–117.
(21) Cronin, J. R.; Pizzarelo, S.; Cruikshank, D. P. In *Meteorites and the Early Solar System*; Kerridge, J., Matthews, M., Eds.; University of Arizona Press: Tucson, 1988; pp 819–857.
(22) Work in progress in collaboration with P. Buseck, Arizona State University, Tempe, AZ.
(23) Anders, E.; Kerridge, J. F. In *Meteorites and the Early Solar System*; Kerridge, J., Matthews, M., Eds.; University of Arizona Press: Tucson, 1988; pp 1155–1186.
(24) Van Schmus, W. R.; Wood, J. A. *Geochim. Cosmochim. Acta* **1967**, *31*, 747–765.
(25) Sears, D. W. G.; Dodd, R. T. In *Meteorites and the Early Solar System*; Kerridge, J., Matthews, M., Eds.; University of Arizona Press: Tucson, 1988; pp 3–31.
(26) Hutchison, R.; Alexander, C. M. O'D.; Barber, D. J. *Geochim. Cosmochim. Acta* **1987**, *51*, 1875–1882.
(27) Alexander, C. M. O'D.; Barber, D. J.; Hutchison, R. *Geochim. Cosmochim. Acta* **1989**, *53*, 3045–3057.
(28) McSween, H. Y., Jr.; Sears, D. W. G. In *Meteorites and the Early Solar System*; Kerridge, J., Matthews, M., Eds.; University of Arizona Press: Tucson, 1988; pp 102–113.
(29) Miyamoto, M.; Fujii, N.; Takeda, H. *Lunar Planet. Sci.* **1981**, *12*, 1145–1152.
(30) Zolensky, M.; McSween, H. Y., Jr. In *Meteorites and the Early Solar System*; Kerridge, J., Matthews, M., Eds.; University of Arizona Press: Tucson, 1988; pp 114–143.
(31) Alexander, C. M. O'D.; Arden, J. W.; Ash, R. D.; Pillinger, C. T. *Earth Planet. Sci. Lett.* **1990**, *99*, 220–229.
(32) Grady, M. M. Private communcation. The Open University, Milton Keynes, U.K.
(33) Hayes, J. M.; Biemann, K. *Geochim. Cosmochim. Acta* **1968**, *32*, 239–267.
(34) Oró, J.; Gilbert, J.; Lichtenstein, H.; Wikstrom, S.; Flory, D. A. *Nature* **1971**, *230*, 105–106.
(35) Pering, K. L.; Ponnamperuma, C. *Science* **1971**, *173*, 237–239.
(36) Hayatsu, R.; Matsuoka, S.; Scott, R. G.; Studier, M. H.; Anders, E. *Geochim. Cosmochim. Acta* **1977**, *41*, 1325–1339.
(37) Tingle, T. N.; Becker, C. H.; Malhotra, R. *Meteoritics* **1991**, *26*, 117–128.
(38) de Vries, M. S.; Wendt, H. R., Hunziker, H. *Lunar Planet. Sci.* **1991**, *XXII*, 315–316.
(39) Hahn, L. H.; Zenobi, R.; Bada, J. L.; Zare, R. N. *Science* **1988**, *239*, 1523–1525.
(40) Zenobi, R.; Philippoz, J.-M.; Buseck, P. R.; Zare, R. N. *Science* **1989**, *246*, 1026–1029.
(41) Wiley, W. C.; McLaren, I. H. *Rev. Sci. Instrum.* **1955**, *26*, 1150–1157.
(42) Mamyrin, B. A.; Kartaev, V. I.; Shmikk, D. V.; Zagulin, V. A. *Sov. Phys.—JETP (Eng. Transl.)* **1973**, *37*, 45.
(43) Buceneli, J. R. Master's Thesis, Stanford University, 1990.
(44) Zenobi, R.; Philippoz, J.-M.; Zare, R. N.; Wing, M. R.; Bada, J. L.; Martl, K. Submitted for publication in *Geochim. Cosmochim. Acta*.
(45) Bandurski, E. L.; Nagy, B. *Geochim. Cosmochim. Acta* **1976**, *40*, 1397–1406.
(46) Tissot, B. P.; Welte, D. H. *Petroleum Formation and Occurrence*; Springer-Verlag: Berlin, 1978; pp 138–141.
(47) Hayatsu, R.; Winans, R. E.; Scott, R. G.; McBeth, R. L.; Moore, L. P.; Studier, M. H. *Science* **1980**, *207*, 1202–1204.
(48) Hayatsu, R.; Scott, R. G.; Winans, R. E. *Meteoritics* **1983**, *18*, 310.
(49) Alfvén, H.; Arrhenius, G. *Evolution of the Solar System*; National Aeronautics and Space Administration: Washington, DC, **1976**; pp 339–366.
(50) Larimer, J. W. *Astrophys. Space Sci.* **1979**, *65*, 351.
(51) Amari, S.; Anders, E.; Virag, A.; Zinner, E. *Nature* **1990**, *345*, 238–240.
(52) Larimer, J. W.; Wasson, J. T. In *Meteorites and the Early Solar System*; Kerridge, J., Matthews, M., Eds.; University of Arizona Press: Tucson, 1988; pp 418–421.
(53) McSween, H. J.; Sears, D. W. G.; Dodd, R. T. In *Meteorites and the Early Solar System*; Kerridge, J., Matthews, M., Eds.; University of Arizona Press: Tucson, 1988; pp 108–109.
(54) Tissot, B. P.; Welte, D. H. *Petroleum Formation and Occurrence*; Springer-Verlag: Berlin, 1978; pp 207–213.
(55) Grady, M. M.; Wright, I. P.; Pillinger, C. T. *Meteoritics* **1989**, *24*, 147–154.
(56) Alexander, C. M. O'D.; Arden, J. W.; Ash, R. D.; Pillinger, C. T. *Earth Planet. Sci. Lett.* **1990**, *99*, 220–229.
(57) Alexander, C. M. O'D.; Arden, J. W.; Pillinger, C. T. *Lunar Planet. Sci.* **1989**, *20*, 7–8.
(58) Shock, E. L.; Schulte, M. D. *Nature* **1990**, *343*, 728–731.

RECEIVED for review September 19, 1991. Accepted December 16, 1991.